ChemComm

COMMUNICATION

View Article Online
View Journal | View Issue

Cite this: *Chem. Commun.*, 2023, **59**, 12184

Received 4th September 2023,
Accepted 20th September 2023

DOI: 10.1039/d3cc04374f

rsc.li/chemcomm

Accurate quantification of DNA content in DNA hydrogels prepared by rolling circle amplification†

Leonie Schneider,[a] Madleen Richter,[a] Claude Oelschlaeger,[b] Kersten S. Rabe,[a] Carmen M. Domínguez[a] and Christof M. Niemeyer*[a]

Accurate quantification of polymerized DNA in rolling circle amplification (RCA)-based hydrogels is challenging due to the high viscosity of these materials, however, it can be achieved with a photometric nucleotide depletion assay or qPCR. We show that the DNA content strongly depends on the template sequence and correlates with the mechanical properties of the hydrogels.

DNA hydrogels have recently attracted great interest because of their porous 3D structure with high water content, tissue-like elastic properties, and the ability to be programmed very efficiently *via* their nucleic acid sequence to install, for example, shape memory persistence, molecular recognition capabilities, and stimulus sensitivity, making them attractive materials for applications in biomedicine, sensing, catalysis, and materials science.[1] Among the numerous methods for the preparation of DNA hydrogels, usually based on self-assembly of synthetic linear or branched DNA motifs, often with the aid of enzymatic ligations or hybridization chain reaction, rolling circle amplification (RCA) plays a special role because of the comparatively low cost of synthetic oligonucleotides required.[2] RCA produces long concatemer single-stranded DNA (ssDNA) chains (>20 000 nt) starting from a short circular ssDNA template using the enzyme phi29 DNA polymerase, which, due to its markedly high processivity, enables the inexpensive production of large quantities of DNA under isothermal conditions.[3] In contrast to hybridization-based DNA hydrogels, where the DNA content can be estimated from the initial DNA monomer concentrations assuming complete hybridization efficacy,[4] the DNA produced by RCA cannot be easily measured. It is noteworthy that so far there is no generic method to accurately quantify the DNA content of RCA hydrogels, but these materials are mainly characterized by their mechanical properties.[5] Several methods have been developed to detect and monitor the RCA process based on labeled hybridization probes or electrophoresis but do not provide information on the accurate amount of DNA.[6] However, quantifiability is of paramount importance for the rational design of DNA hydrogels and a comprehensive understanding of the RCA process in order to (i) investigate the influence of fundamental parameters of the RCA process, (ii) achieve consistent, reproducible, and predictable materials properties, or (iii) adjust the stoichiometric ratios of components in DNA hybrid materials to improve applications.

Although quantitative PCR (qPCR) is the well-established gold standard for accurate DNA quantification[7] that is also used in DNA nanotechnology,[8] to our knowledge this method has never been applied for quantification of DNA in RCA hydrogels. One explanation why qPCR has not been used so far could be the high viscosity of these materials resulting from the entanglement of the ultra-long DNA chains within the 3D network,[2] which methodologically complicates a clean qPCR analysis. To address this issue, we report here the evaluation of different methodologies for their suitability for accurate quantification of amplified DNA in RCA hydrogels, based on the fundamental question of whether different circular templates with different DNA sequence lead to different RCA efficiencies. While there is strong evidence that the sequence composition can significantly affect the RCA efficiency, one related work has only performed relative comparisons of the amount of product.[6d] Here we compare two methods based on either the use of a double-strand sensitive intercalator dye or, for the first time, photometric quantification of nucleotides present in the reaction mixture with the qPCR method for their capability for accurate quantification of amplified DNA in RCA hydrogels.

In order to identify suitable methods for accurate quantification of DNA in RCA-based hydrogels, we performed a time-resolved study of the RCA process as a function of three literature-proven templates that differ in their DNA sequence and thus their ability to form secondary structures by intramolecular base pairing. Sequences of templates A and B were

[a] *Institute of Biological Interfaces (IBG-1), Karlsruhe Institute of Technology (KIT), Hermann-von-Helmholtz Platz 1, 76344 Eggenstein-Leopoldshafen, Germany. E-mail: niemeyer@kit.edu*
[b] *Institute for Mechanical Process Engineering and Mechanics, Karlsruhe Institute of Technology (KIT), Gotthard-Franz-Straße 3, 76131 Karlsruhe, Germany*

† Electronic supplementary information (ESI) available. See DOI: https://doi.org/10.1039/d3cc04374f

designed by the Walther group for the preparation of mechanosensitive RCA hydrogels,[9] while sequence C contains stem loops and restriction sites, originally designed by the Tan group[10] and used by us for the preparation of DNA nanocomposite materials.[11] The three sequences A–C were purchased as linear oligonucleotides from a commercial supplier and converted into circularized templates by enzymatic ligation. (Fig. S1 and S2, ESI†). In the typical experimental workflow, the templates were then used for RCA reactions in a total reaction volume of 250 μL using a short primer, phi29 polymerase and dNTPs. Samples were taken at different time points within the total reaction time of 72 h.

Fluorometric Sybr Green assay. We first tested a simple quantification approach using the nucleic acid dye Sybr Green I (Thermo Fisher Scientific). The emitted fluorescence of Sybr Green I increases dramatically (>1000-fold) upon incorporation into double-stranded DNA, resulting in high detection sensitivity and usability in bioanalytical assays such as real-time PCR.[12] During RCA, phi29 polymerase continuously amplifies the complementary sequence of the circular template, generating long ssDNA chains that can subsequently assemble into more energetically favourable secondary structures by intramolecular base pairing. Quantification of secondary structures during RCA should therefore allow conclusions to be drawn about the total amount of DNA present and could also provide insights into amplification kinetics, as has been demonstrated in other applications.[13] To prevent an inhibitory effect of the intercalating dye on polymerase efficiency, which has been observed in other PCR systems,[14] we did not use Sybr Green I *in situ* during the RCA reaction, but added it after the reaction. The amplification process was stopped by heat denaturation of phi29 polymerase, Sybr Green I was added by thorough pipetting of the reaction mixture, and fluorescence intensity was measured at λ_{Em} = 520 nm (Fig. S4, ESI†). The general workflow is shown in Fig. 1A. The measured fluorescence signals were correlated with the absolute amount of DNA in the sample using a calibration curve generated with herring sperm DNA of known concentration (Fig. S3, ESI†). The resulting quantitative DNA amounts in the standard reaction volume of 250 μL at different reaction time points are shown in Fig. 1C.

Data from the Sybr Green I assay suggested that after a reaction time of 72 hours, all three templates resulted in similar amounts of double-stranded DNA in the range of 3–4 μg. However, it needs to be taken into account that this assay is highly dependent on the template-dependent formation of secondary structures, as the binding of Sybr Green I to ssDNA is at least 11-fold lower compared to dsDNA.[12a] To determine differences in the structure of the RCA products, we performed a secondary structure analysis of the complementary sequences (A′, B′, C′) formed by RCA from the different circular templates using the software mfold[15] (Fig. 1B, for the detailed analysis of the secondary structure prediction, see Fig. S5 and S6, ESI†). From the analysis, it is evident that the secondary structure of amplicon C′ has the lowest free energy compared to sequences A′ and B′ due to the formation of a long stem loop, which should significantly increase the incorporation efficiency

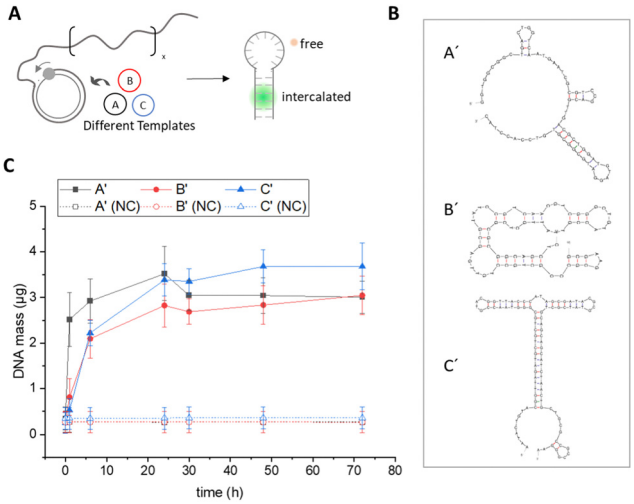

Fig. 1 Quantification of amplified DNA using Sybr Green I. (A) Concatemers generated from circular templates A–C during RCA form secondary structures that are detected with the intercalating dye Sybr Green I and quantified using a calibration curve (Fig. S3, ESI†). (B) Prediction of the amplicon secondary structures of templates A–C using mfold web server (see also Fig. S5 and S6, ESI†). (C) Total DNA mass (μg) in a 250 μL RCA reaction as determined with Sybr Green. Negative controls (NC) were carried out in the absence of phi29 polymerase. Error bars indicate the standard deviation from three independent experiments.

of the Sybr Green I dye. Therefore, due to the strong dependence of Sybr Green I fluorescence on the structural nature of the DNA to be detected, this assay did not seem suitable for comparative sequence-dependent or accurate quantitative studies of the RCA process.

Photometric supernatant depletion assay. As an alternative method for accurate DNA quantification that does not depend on sequence-specific features such as secondary structure, we developed a supernatant depletion assay based on photometric detection of deoxynucleotide triphosphate (dNTP) building blocks (Fig. 2). As shown in Fig. 2A, RCA was performed using the different templates, and samples were collected at different time points, from which the supernatant was separated from the viscous polymeric DNA hydrogel by ultrafiltration using a filter membrane with a molecular weight cut-off of 10 kDa, which effectively separates all oligomers >30 nucleotides (nt). By measuring the concentration of dNTP in the filtrate by UV/vis spectroscopy at λ_{Abs} = 260 nm and correlating the values obtained with those at the start point before RCA, the amount of dNTP incorporated into the DNA polymer could be calculated (see also experimental section in the ESI†). As expected, the depletion assay showed a continuous decrease of dNTPs in the supernatant during the course of RCA, indicating the formation of RCA products over time (Fig. 2B). Comparison of the three templates A, B, and C revealed clear differences in dNTP consumption. For sequence A′ about half of the dNTPs were consumed after a reaction time of 72 h, whereas for the other two sequences less than a quarter of the available dNTPs were incorporated into the RCA products.

This indicated a strong dependence of RCA productivity on template sequence. The exact total mass of DNA produced was

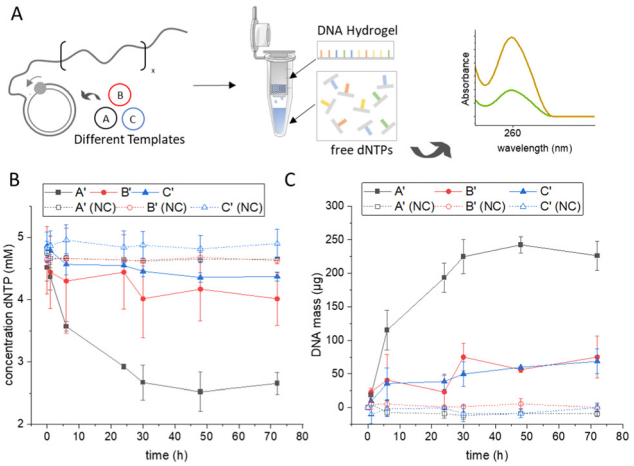

Fig. 2 Quantification of amplified DNA by photometric measurement of nucleotide depletion. (A) During the RCA process, nucleotides are consumed by phi29 polymerase to generate long ssDNA. The viscous DNA hydrogel and long DNA oligomers (> 30 nt) are separated by filtration and the free nucleotides in the filtrate are quantified by UV/vis spectroscopy. (B) Concentration of free nucleotides in the supernatant at varying time points of RCA. (C) Total DNA mass (µg) in a 250 µL RCA reaction mixture calculated from the consumed nucleotides. Negative controls (NC) were carried out in the absence of phi29 polymerase. Error bars in (B) and (C) indicate the standard deviation from three independent experiments. Note that amplification reaches a plateau phase after approximately 48 h, presumably due to the instability of phi29 polymerase over extended periods of time.

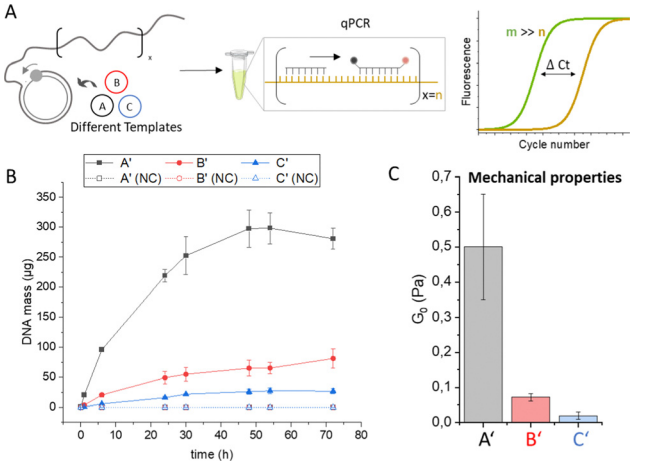

Fig. 3 Quantification of DNA using qPCR. (A) RCA amplicons are quantified using a TaqMan probe containing a fluorescent reporter and a quencher dye, which are separated during amplification by the Taq polymerase. The fluorescence signal is correlated with background fluorescence and plotted as a ΔCt value that indicates at which PCR cycle the measurement signal appears compared to the background. (B) Total DNA mass (µg) in a 250 µL RCA reaction mixture as determined by qPCR using a calibration curve of the respective amplicon sequence (Fig. S8, ESI†). Negative controls (NC) were carried out in the absence of phi29 polymerase. Error bars indicate the standard deviation from three independent experiments. (C) Mechanical properties of DNA hydrogels after 72 h RCA polymerization determined by bulk rheology. The elastic plateau modulus G_0 was determined by frequency sweep analysis (Fig. S11 and S12, ESI†).

calculated from the determined dNTP consumptions, taking into account the reaction volume and the specific molecular weight of the nucleotides consumed (Fig. 2C). Template A caused a significantly higher polymerase efficiency and resulted in more than twice the amount of DNA as templates B and C, which in turn showed very similar values for that of total DNA production. Attempts were also made to gravimetrically determine the amount of substance in the hydrogel formed by weighing out the filter membrane, but this resulted in inconsistent values and large error bars, likely due to the low absolute masses of the RCA products compared to the net weight of the ultrafiltration cup (Fig. S7, ESI†). Overall, the new spectroscopic method not only showed good sensitivity and reliability in DNA quantification of RCA hydrogels but, moreover, was independent of the structural features of the template because it relies only on the dNTP consumption.

Quantitative polymerase chain reaction. To validate the newly developed photometric assay, we aimed to analyse the RCA process by qPCR. the gold standard for DNA quantification.[7] In qPCR, a fluorescently labelled probe is used to measure the concentration of a target sequence (Fig. 3A). In establishing a suitable qPCR protocol to quantify the amount of DNA in the RCA hydrogels, we encountered technical difficulties resulting from the viscous, gel-like consistency of the RCA samples, which leads to the formation of filaments during pipetting (Fig. S2B, ESI†). This leads to inhomogeneous DNA distribution during aliquoting and preparation of qPCR samples, resulting in high error bars and unreliable qPCR results (Fig. S9A, ESI†). To achieve homogeneous DNA distribution in the RCA samples, we treated the RCA products with ultrasound, a standard method used in genome research to fragment very long genomic DNA samples, which produces fragments of a few hundred bases and does not cause significant artifacts in qPCR.[16] Indeed, the ultrasonication led to fragmentation of the long, entangled ssDNA chains, thereby reducing the viscosity of the samples and allowing a satisfactory qPCR analysis that showed low error bars for all three sequences (Fig. S9B and Fig. 3C, ESI†). The obtained data revealed clear differences in template-dependent DNA polymer evolution (Fig. 3C), similar as observed in Fig. 2C. Template A led to significantly higher DNA amounts after several hours than templates B and C. In the case of sequences A and B, the absolute DNA amounts in the qPCR were similar to those of the dNPT depletion assay (sequence A′: 281 ± 17 µg and 226 ± 22 µg for the qPCR and dNPT assays, respectively; sequence B′: 81 ± 31 µg or 75 ± 16 µg, respectively), whereas a difference was observed for sequence C′ (27 ± 4 µg or 68 ± 18 µg, respectively). In addition, qPCR analysis confirmed that amplification reaches plateau phase after approximately 48 h, which is likely due to the half-life of phi29 polymerase activity.[17] Statistical significance tests showed that of all three quantification methods examined, only the qPCR assay yielded significant differences in the quantified amount of amplified DNA (Fig. S10, ESI†). The rheological properties of hydrogels A′, B′, C′ obtained after 72 h RCA reaction time were also characterized (Fig. S11 and S12, ESI†). The analyses showed that the viscoelastic properties of the DNA

hydrogel samples follow the same trend observed by qPCR for sequence-dependent DNA quantification. In particular, the elasticity of the hydrogels, characterized by the elastic plateau modulus G_0, decreased continuously with $G_0 = 0.50 \pm 0.15$ Pa, 0.07 ± 0.01 Pa and 0.02 ± 0.01 Pa for hydrogels with sequences A′, B′ and C′, respectively (Fig. 3C). The correlation of qPCR and rheology data indicates a strong dependency of the material properties from the DNA content. Given the central role that material properties play in the development of RCA hydrogels, we believe that too little emphasis has been placed on the quantitative characterization of these highly viscous materials.

The question remains as to the reason for the strong sequence dependence of productivity. Secondary structures likely play a role, which can slow down many polymerases.[18] Although phi29 polymerase exhibits a high strand displacement ability,[19] the resolution of secondary structures could lower elongation rates,[20] so that enzyme and substrate half-lives become limiting. Moreover, the template's nucleotide composition can affect reaction rates, as many polymerases have different incorporation rates for different nucleotides.[18] For phi29 polymerase, a study suggested selectivity for DNA templates rich in adenosine (A) and cytidine (C), but secondary structures were not considered.[6d] In our case, templates A, B and C have an AC content of 58.3%, 54.1% and 50%, respectively. While the observed trend of RCA efficiency might correlate with the template's AC content, we believe that differences in the secondary structures of templates and RCA products play a more decisive role here. Hence, further systematic studies are needed to shed more light on the individual factors affecting the process of RCA-based hydrogel production.

In summary, we established two feasible methods for accurate DNA quantification in RCA-based DNA hydrogels that do not depend on the secondary structure of the amplicons. The dNTP depletion assay showed higher experimental uncertainties, whereas the qPCR assay proved to be reliable and easy to use. Using qPCR, we found that RCA amplification rate strongly depends on the template sequence and has a strong effect on the mechanical properties of the resulting materials. We believe that the methodology presented here is a powerful tool as it combines high throughput with low resource requirements and allows the systematic study of reaction parameters to gain better access to the rational design of RCA materials.

This work was financially supported through the Helmholtz program ''Materials Systems Engineering'' under the topic ''Adaptive and Bioinstructive Materials Systems'', DFG (GRK2039) and the BMBF project 161L0284A MicroMatrix.

Conflicts of interest

There are no conflicts to declare.

Notes and references

1 (*a*) D. Yang, M. R. Hartman, T. L. Derrien, S. Hamada, D. An, K. G. Yancey, R. Cheng, M. Ma and D. Luo, *Acc. Chem. Res.*, 2014, **47**, 1902–1911; (*b*) J. Li, L. Mo, C.-H. Lu, T. Fu, H.-H. Yang and W. Tan, *Chem. Soc. Rev.*, 2016, **45**, 1410–1431; (*c*) D. Wang, Y. Hu, P. Liu and D. Luo, *Acc. Chem. Res.*, 2017, **50**, 733–739; (*d*) Y. Hu and C. M. Niemeyer, *Adv. Mater.*, 2019, **31**, e1806294; (*e*) M. Vázquez-González and I. Willner, *Angew. Chem., Int. Ed.*, 2020, **59**, 15342–15377; (*f*) V. Morya, S. Walia, B. B. Mandal, C. Ghoroi and D. Bhatia, *ACS Biomater. Sci. Eng.*, 2020, **6**, 6021–6035; (*g*) J. Gačanin, C. V. Synatschke and T. Weil, *Adv. Funct. Mater.*, 2020, **30**, 1906253.
2 J. B. Lee, S. Peng, D. Yang, Y. H. Roh, H. Funabashi, N. Park, E. J. Rice, L. Chen, R. Long, M. Wu and D. Luo, *Nat. Nanotechnol.*, 2012, **7**, 816.
3 (*a*) L. Blanco, A. Bernad, J. M. Lázaro, G. Martín, C. Garmendia and M. Salas, *J. Biol. Chem.*, 1989, **264**, 8935–8940; (*b*) S. Kamtekar, A. J. Berman, J. Wang, J. M. Lázaro, M. de Vega, L. Blanco, M. Salas and T. A. Steitz, *Mol. Cell*, 2004, **16**, 609–618.
4 S. H. Um, J. B. Lee, N. Park, S. Y. Kwon, C. C. Umbach and D. Luo, *Nat. Mater.*, 2006, **5**, 797–801.
5 C. Yao, R. Zhang, J. Tang and D. Yang, *Nat. Protoc.*, 2021, **16**, 5460–5483.
6 (*a*) M. Nilsson, M. Gullberg, F. Dahl, K. Szuhai and A. K. Raap, *Nucleic Acids Res.*, 2002, **30**, e66; (*b*) M. M. Ali, S. Su, C. D. M. Filipe, R. Pelton and Y. Li, *Chem. Commun.*, 2007, 4459–4461; (*c*) H.-X. Jiang, M.-Y. Zhao, C.-D. Niu and D.-M. Kong, *Chem. Commun.*, 2015, **51**, 16518–16521; (*d*) Y. Mao, M. Liu, K. Tram, J. Gu, B. J. Salena, Y. Jiang and Y. Li, *Chem. Eur. J.*, 2015, **21**, 8069–8074; (*e*) L. Xu, J. Duan, J. Chen, S. Ding and W. Cheng, *Anal. Chim. Acta*, 2021, **1148**, 238187.
7 S. C. Taylor, K. Nadeau, M. Abbasi, C. Lachance, M. Nguyen and J. Fenrich, *Trends Biotechnol.*, 2019, **37**, 761–774.
8 (*a*) C. Timm and C. M. Niemeyer, *Angew. Chem., Int. Ed.*, 2015, **54**, 6745–6750; (*b*) S. Dey, C. Fan, K. V. Gothelf, J. Li, C. Lin, L. Liu, N. Liu, M. A. D. Nijenhuis, B. Saccà, F. C. Simmel, H. Yan and P. Zhan, *Nat. Rev. Dis. Primers*, 2021, **1**, 13.
9 R. Merindol, G. Delechiave, L. Heinen, L. H. Catalani and A. Walther, *Nat. Commun.*, 2019, **10**, 528.
10 G. Zhu, R. Hu, Z. Zhao, Z. Chen, X. Zhang and W. Tan, *J. Am. Chem. Soc.*, 2013, **135**, 16438–16445.
11 (*a*) Y. Hu, C. M. Domínguez, J. Bauer, S. Weigel, A. Schipperges, C. Oelschlaeger, N. Willenbacher, S. Keppler, M. Bastmeyer, S. Heißler, C. Wöll, T. Scharnweber, K. S. Rabe and C. M. Niemeyer, *Nat. Commun.*, 2019, **10**, 5522; (*b*) Y. Hu and C. M. Niemeyer, *J. Mater. Chem. B*, 2020, **8**, 2250–2255; (*c*) Y. Hu, D. Rehnlund, E. Klein, J. Gescher and C. M. Niemeyer, *ACS Appl. Mater. Interfaces*, 2020, **12**, 14806–14813.
12 (*a*) H. Zipper, H. Brunner, J. Bernhagen and F. Vitzthum, *Nucleic Acids Res.*, 2004, **32**, e103–e103; (*b*) A. I. Dragan, R. Pavlovic, J. B. McGivney, J. R. Casas-Finet, E. S. Bishop, R. J. Strouse, M. A. Schenerman and C. D. Geddes, *J. Fluoresc.*, 2012, **22**, 1189–1199.
13 R. G. Rutledge and D. Stewart, *BMC Biotechnol.*, 2008, **8**, 47.
14 K. Nath, J. W. Sarosy, J. Hahn and C. J. Di Como, *J. Biochem. Biophys. Methods*, 2000, **42**, 15–29.
15 M. Zuker, *Nucleic Acids Res.*, 2003, **31**, 3406–3415.
16 (*a*) T. L. Mann and U. J. Krull, *Biosens. Bioelectron.*, 2004, **20**, 945–955; (*b*) S. G. Acinas, R. Sarma-Rupavtarm, V. Klepac-Ceraj and M. F. Polz, *Appl. Environ. Microbiol.*, 2005, **71**, 8966–8969.
17 T. Povilaitis, G. Alzbutas, R. Sukackaite, J. Siurkus and R. Skirgaila, *Protein Eng., Des. Sel.*, 2016, **29**, 617–628.
18 J. L. Montgomery, N. Rejali and C. T. Wittwer, *J. Mol. Diagn.*, 2014, **16**, 305–313.
19 J. A. Morin, F. J. Cao, J. M. Lázaro, J. R. Arias-Gonzalez, J. M. Valpuesta, J. L. Carrascosa, M. Salas and B. Ibarra, *Proc. Natl. Acad. Sci. U. S. A.*, 2012, **109**, 8115–8120.
20 M. a S. Soengas, C. Gutiérrez and M. Salas, *J. Mol. Biol.*, 1995, **253**, 517–529.